A numerical investigation of properties of the electronic self-energy potential for metallic systems

1990 J. Phys.: Condens. Matter 2 1537

(http://iopscience.iop.org/0953-8984/2/6/013)

J. Phys.: Condens. Matter 2 (1990) 1537–1548. Printed in the UK

A numerical investigation of properties of the electronic self-energy potential for metallic systems

D P Joubert† and J C Inkson
Physics Department, University of Exeter, Stocker Road, Exeter EX4 4QL, UK

Received 7 August 1989

Abstract. We examine some properties of the electronic self-energy potential for metallic systems within the GW–plasmon-pole approximation. The self-energy is found to be highly state dependent. States with bonding character are depressed relative to states with less bonding character when compared to density functional eigenenergies, irrespective of whether they are occupied or not.

1. Introduction

Understanding the electronic properties of systems of electrons and ions is central to solid state physics, yet despite all the effort that has been devoted to the subject there remains much detail to be unravelled about electronic interactions. Since the sixties, density functional theory (DFT) [1] in its local approximation has been the conventional way to describe electronic structure in solids. DFT has been very successful in accounting for ground-state properties, and although DFT eigenvalues have no obvious physical meaning, they are widely interpreted as single-particle excitation energies. Only the formal resemblance between the DFT expression and the many-body expression for quasiparticle properties [2] lends some credence to this interpretation. It is somewhat surprising that there even exists such a good qualitative correspondence between DFT eigenvalues and measured single-particle excitations. In DFT, a local potential (the exchange–correlation potential) common to all one-electron states is designed to generate the correct ground-state density. It is too much to expect that this potential will also describe the exact physical nature of the band structure [3].

The so-called band-gap problem for insulators and semiconductors is an obvious example where DFT has to be interpreted carefully [3–6]. Perdew and Levy [3] and Sham and Schlüter [4] showed that there is a discontinuity in the derivative of the DFT exchange–correlation potential V_{xc} on adding a hole or electron to the ground state. The DFT band gap differs from the difference between the lowest unoccupied state and the highest occupied state for the N-body system by the discontinuity in V_{xc} on adding an electron to the N-body system. In the local density approximation to V_{xc} there is no discontinuity in the exchange–correlation potential, but in a numerical study by Godby, Schlüter and Sham [7], it was shown that even 'true' DFT still underestimates the measured band-gap

† Permanent address: Physics Department, University of the Witwatersrand, PO Wits, Johannesburg 2050, South Africa.

0953-8984/90/061537 + 12 $03.50

energy and that this is therefore an intrinsic property of DFT, not a feature of the local density approximation. Recent calculations [7–9] demonstrated that reasonable band gaps can be calculated within the GWA–RPA approximation to the quasiparticle expression. These calculations demonstrated that the dispersion of the bands cannot be reproduced by a state and energy independent potential, since such a potential excludes some essential physics (see also [10–12]). This conclusion was reached as early as 1971 by Kane and others [38, 39].

In recent years as experimental and theoretical techniques improved, differences between experimental and theoretical results for metals became more obvious as well, and the need for a more complete theoretical treatment became clear. Accurate measurements of band widths in simple metals, for example [13–16], showed a considerable deviation from predicted values. Studies in the late sixties [17–21] showed that electron–electron interactions in a homogeneous electron gas at metallic densities lead to band-width narrowing, but the effect was not large enough to account for differences between DFT and experimetnal results. This stimulated a number of theoretical attempts [14, 21–27] to improve the prediction of the band width. Discrepancies between theory and experiment for transition metals have also long been known (see L C Davis for references [29]). Simple local approximations to the self-energy [28] improved the results, but significant differences remain.

In most of the theoretical studies, the GW approximation with neglect of vertex corrections was used. Vertex corrections describe the correlation between the position of an electron and the positions of electrons in the local screening charge. Neglect of vertex corrections can lead to unphysical results. An example is the pair correlation function in a homogeneous electron gas which becomes negative at short separations when vertex corrections are neglected. Northup and Louie [22], Surh, Northrup and Louie [23] and Lyo and Plummer [14] found that the inclusion of vertex corrections in the screened Coulomb interaction increases the band-width reduction in alkali metals. In a recent publication, Mahan and Sernelius [27] demonstrated that the inclusion of vertex corrections in both the numerator of the self-energy and the dielectric function nearly cancel, returning the results to values close to those of the GW–RPA calculation. In some of the recent calculations [8, 22] the real part of the self-energy is obtained by solving Dyson's equation for the Green function. Lifetime effects (imaginary part of the self-energy) are neglected. Reasonable results are only obtained if the internal undressed Green functions are replaced by dressed ones. This is done in an approximate way by replacing the unperturbed energies in the Green function by the perturbed ones and iterating to self-consistency. Rice [20] argued that this is effectively equivalent to summing over an infinite class of self-energy diagrams but that in the above procedure important diagrams are multiply counted. It is therfore difficult to decide how good the results obtained are.

In this paper we do not attempt to address the uncertainties surrounding the GW approximation, but based on the success achieved using this approximation [7–10, 22–23] we take it as a good starting point for examining some of the properties of the self-energy potential for a number of model systems in a qualitative way. In semiconductors and insulators there is a discontinuity in the self-energy between the valence and conduction bands. This feature is absent when the difference in symmetry between the valence and conduction band states is not taken into account [12, 28]. Here we investigate the state and energy dependence of the GW self-energy for metallic systems.

In section 2 we discuss the theoretical model. In section 3 some numerical details are summarised, while the results for a number of model systems are presented in section 4. Finally in section 5 we summarise and discuss the work presented in this paper.

2. Theoretical model

In the Green function formalism [2] the N-particle Schrödinger equation reduces to a quasiparticle expression:

$$h_0(\boldsymbol{r}) + \int \mathrm{d}\boldsymbol{r}\, \Sigma(\boldsymbol{r}, \boldsymbol{r}', \varepsilon^{\mathrm{qp}})\psi(\boldsymbol{r}') = \varepsilon^{\mathrm{qp}}\psi(\boldsymbol{r}). \tag{1}$$

The Hartree Hamiltonian $h_0(\boldsymbol{r})$ contains contributions from the kinetic energy, the external potential and the Hartree potential. The self-energy $\Sigma(\boldsymbol{r}, \boldsymbol{r}', \omega)$ is a non-local, energy dependent non-Hermitian operator. Due to the non-Hermiticity of the Hamiltonian, the quasiparticle energies are in general complex. The real part is related to the excitation energies, and the imaginary part is related to the finite lifetime of the excitations. The quasiparticle functions $\psi(\boldsymbol{r})$ form a complete set of states, but in general are neither normalised nor linearly independent. $\Sigma(\boldsymbol{r}, \boldsymbol{r}', \omega)$ is related via a coupled set of integral equations to the Green function

$$G(\boldsymbol{r}, \boldsymbol{r}', \omega) = \sum_{\alpha} \frac{\psi_{\alpha}^{\mathrm{qp}}(\boldsymbol{r})^* \psi_{\alpha}^{\mathrm{qp}}(\boldsymbol{r}')}{\omega - \varepsilon_{\alpha}^{\mathrm{qp}} - \mathrm{i}\delta\, \mathrm{sgn}(\varepsilon_{\mathrm{F}} - \varepsilon_{\alpha}^{\mathrm{qp}})} \tag{2}$$

the screened Coulomb interaction

$$W(\boldsymbol{r}, \boldsymbol{r}', \omega) = \int \mathrm{d}\boldsymbol{r}''\, \varepsilon^{-1}(\boldsymbol{r}, \boldsymbol{r}'', \omega) v(\boldsymbol{r}'', \boldsymbol{r}') \tag{3}$$

and the vertex function

$$\Gamma = 1 + \delta\Sigma/\delta V. \tag{4}$$

Here ε_F stands for the Fermi energy, $v(\boldsymbol{r} - \boldsymbol{r}')$ denotes the bare Coulomb interaction and $\varepsilon(\boldsymbol{r}, \boldsymbol{r}', \omega)$ is the dielectric matrix. In the GW approximation vertex corrections are neglected. This corresponds to the first-order term in a series expansion of the self-energy in terms of the screened interaction W, leading to the expression for the self-energy

$$\Sigma(\boldsymbol{r}, \boldsymbol{r}', \omega) = \frac{1}{2\pi\mathrm{i}} \int \mathrm{d}\omega'\, \mathrm{e}^{\mathrm{i}\delta^+\omega'}\, G(\boldsymbol{r}, \boldsymbol{r}', \omega - \omega') W(\boldsymbol{r}', \boldsymbol{r}, \omega') \tag{5}$$

where δ^+ is an infinitesimal positive number. The same approximation for the dielectric matrix leads to the random-phase approximation (RPA)

$$\varepsilon(\boldsymbol{r}, \boldsymbol{r}', \omega) = \delta(\boldsymbol{r} - \boldsymbol{r}') + \frac{1}{2\pi\mathrm{i}} \int \mathrm{d}\boldsymbol{r}''\, \mathrm{d}\omega'\, v(\boldsymbol{r} - \boldsymbol{r}'') G(\boldsymbol{r}, \boldsymbol{r}'', \omega - \omega') G(\boldsymbol{r}'', \boldsymbol{r}', \omega'). \tag{6}$$

For metallic systems, few attempts have been made to calculate the dielectric matrix for realistic systems even in RPA. In this work we model the dielectric matrix following a procedure suggested by Hybertsen and Louie [30]. We write the screened interaction as [30]

$$W(\boldsymbol{r}, \boldsymbol{r}', 0) = \tfrac{1}{2}[W^{\mathrm{hom}}(\boldsymbol{r} - \boldsymbol{r}'; r_{\mathrm{s}}(\boldsymbol{r}')) + W^{\mathrm{hom}}(\boldsymbol{r}' - \boldsymbol{r}; r_{\mathrm{s}}(\boldsymbol{r}))] \tag{7}$$

where $r_{\mathrm{s}}(\boldsymbol{r})$ is the local electron density parameter at $\boldsymbol{r}$. The local screening response is

determined by the Lindhard dielectric function for a homogeneous electron gas. The Fourier transform of equation (7) yields

$$\varepsilon^{-1}_{GG'}(\boldsymbol{q},0)=\frac{1}{2}\Big(v(\boldsymbol{q}+\boldsymbol{G})\int \mathrm{d}\boldsymbol{r}\,\varepsilon^{-1}(|\boldsymbol{q}+\boldsymbol{G}|;\boldsymbol{r}_s(\boldsymbol{r}))\exp[\mathrm{i}(\boldsymbol{G}-\boldsymbol{G}')\cdot\boldsymbol{r}]$$

$$+v(\boldsymbol{q}+\boldsymbol{G}')\int \mathrm{d}\boldsymbol{r}\,\varepsilon^{-1}(|\boldsymbol{q}+\boldsymbol{G}'|;\boldsymbol{r}_s(\boldsymbol{r}))\exp[\mathrm{i}(\boldsymbol{G}'-\boldsymbol{G})\cdot\boldsymbol{r}]\Big) \tag{8}$$

where $\boldsymbol{G}$ is a reciprocal lattice vector and $\boldsymbol{q}$ is a vector in the first Brillouin zone. The diagonal terms of ε^{-1} give an average of the local screening response at different points of the Brillouin zone while the off-diagonal terms contain information about local fields or the inhomogeneity of the system. We extend the static response function to finite frequencies using the generalised plasmon-pole model of von der Linden and Horsch [9]. First we symmetrise the static dielectric function to give

$$\tilde{\varepsilon}^{-1}_{GG'}(\boldsymbol{q},0)=\varepsilon^{-1}_{GG'}(\boldsymbol{q},0)|\boldsymbol{q}+\boldsymbol{G}|/|\boldsymbol{q}+\boldsymbol{G}'| \tag{9}$$

and express it in its eigen-representation [30]

$$\tilde{\varepsilon}^{-1}_{GG'}(\boldsymbol{q},0)=\delta_{GG'}+\sum_{i=1}U_{qi}(\boldsymbol{G})(\tilde{\varepsilon}_i^{-1}(\boldsymbol{q})-1)U^*_{qi}(\boldsymbol{G}'). \tag{10}$$

Here $U_{qi}(\boldsymbol{G})$ is the $\boldsymbol{G}$ component of the ith eigenvector of $\tilde{\varepsilon}^{-1}(\boldsymbol{q})$, with corresponding eigenvalue $\tilde{\varepsilon}_i^{-1}(\boldsymbol{q})$. The generalised plasmon-pole approximation at finite frequencies then becomes [9]

$$\tilde{\varepsilon}^{-1}_{GG'}(\boldsymbol{q},\omega)=\delta_{GG'}+\sum_{i=1}U_{qi}(\boldsymbol{G})\left(\frac{z_i(\boldsymbol{q})}{\omega_i^2-(\omega(\boldsymbol{q})-\mathrm{i}\delta)^2}\right)U^*_{qi}(\boldsymbol{G}') \tag{11}$$

where

$$z_i(\boldsymbol{q})=\omega_{\mathrm{pl}}^2\sum_{GG'}\frac{U^*_{qi}(\boldsymbol{G})(\boldsymbol{q}+\boldsymbol{G})\cdot(\boldsymbol{q}+\boldsymbol{G}')U_{qi}(\boldsymbol{G}')}{|\boldsymbol{q}+\boldsymbol{G}||\boldsymbol{q}+\boldsymbol{G}'|} \tag{12}$$

and

$$\omega_i^2(\boldsymbol{q})=z_i(\boldsymbol{q})/(1-\varepsilon_i^{-1}(\boldsymbol{q})). \tag{13}$$

Here $\omega_{\mathrm{pl}}^2=4\pi\rho(0)$ is the free electron plasma frequency at the average ground-state electron density and $\rho(\boldsymbol{G})$ are the components of the Fourier transform of the ground-state charge density. The diagonal terms of $\tilde{\varepsilon}$ satisfy the f-sum rule [2], and the plasmon frequencies (13) are positive since the eigenvalues $\varepsilon_i^{-1}(\boldsymbol{q})$ lie in the interval (0, 1) [31]. Within the GW–plasmon-pole approximation, the self-energy is real for $\varepsilon_F-\omega_{\mathrm{pl}}<\omega<\varepsilon_F+\omega_{\mathrm{pl}}$ for metallic systems and consequently the Hamiltonian (1) is Hermitian in this range of energies.

For a given starting potential $\Sigma_0(\boldsymbol{r},\boldsymbol{r}',\omega)$, equation (1) defines a set of wavefunctions and energies that can be used to construct a new self-energy operator $\Sigma_1(\boldsymbol{r},\boldsymbol{r}',\omega)$. This procedure can be repeated until self-consistency is achieved, but as pointed out in the introduction there is some uncertainty concerning the validity of this approach. In this paper we study some of the differences and similarities between DFT eigenvalues and

quasiparticle energies in a qualitative manner and stop after the first iteration. We start from a DFT Hamiltonian with a given $V(\boldsymbol{r})$:

$$H(\boldsymbol{r}) = T + V(\boldsymbol{r}) \tag{14}$$

where T is the kinetic energy and

$$V(\boldsymbol{r}) = V_{\text{ext}}(\boldsymbol{r}) + V_{\text{H}}(\boldsymbol{r}) + V^{\text{xc}}_{\text{LDF}}(\boldsymbol{r}) \tag{15}$$

with $V_{\text{ext}}(\boldsymbol{r})$ an unspecified external potential, $V_{\text{H}}(\boldsymbol{r})$ the Hartree potential, and $V^{\text{xc}}_{\text{LDF}}(\boldsymbol{r})$ a local approximation to the DFT exchange–correlation potential. For a given $V(\boldsymbol{r})$, equation (14) defines a ground-state charge density from which the Hartree, exchange–correlation and then the external potential can be calculated. Leaving the external potential initially unspecified obviates the need for the self-consistency loop generally required to solve the DFT Hamiltonian. In this work we use the exchange–correlation potential calculated by Hedin [19] in its parameterised form [32]. This is consistent with the GW approximation used in the current study.

Hybertsen and Louie [8] found that the DFT wave functions and quasiparticle functions in their calculations were almost identical, with an overlap of more than 99%. We confirmed this finding in our calculations. Using this fact, the differences between the DFT eigenvalues and quasiparticle energies for a given state in its lowest approximation [9] can be expressed as a single matrix element

$$\Delta\Sigma = \langle \psi^{\text{DFT}}_{\alpha} | \Sigma(\varepsilon^{\text{qp}}_{\alpha}) - V^{\text{xc}}_{\text{DFT}} | \psi^{\text{DFT}}_{\alpha} \rangle. \tag{16}$$

After solving the DFT Hamiltonian (14) we calculate the self-energy using the eigenvalues and eigenfunctions of H, and then solve Dyson's equation to obtain $\varepsilon^{\text{qp}}_{\alpha}$.

The GW–plasmon-pole approximation leads to the following expressions for the self-energy matrix elements in the DFT basis functions:

$$\langle \psi_{kn} | \Sigma^{\text{corr}}(\omega) | \psi_{kn} \rangle = \frac{1}{2} \sum_{l} \frac{1}{V} \sum_{\boldsymbol{q}}^{1\text{BZ}} \sum_{i} \frac{z_i(\boldsymbol{q}) [S^{kn}_{\boldsymbol{q}l}]^* [S^{kn}_{\boldsymbol{q}l}]}{\omega_i(\boldsymbol{q})(\omega - \varepsilon_{k-\boldsymbol{q}l} + \text{sgn}(\varepsilon_{\text{F}} - \varepsilon_{k-\boldsymbol{q}l})\omega_i(\boldsymbol{q}))} \tag{17a}$$

where

$$S^{kn}_{\boldsymbol{q}l} = \int \mathrm{d}\boldsymbol{r}\, \psi^*_{kn}(\boldsymbol{r}) \Phi_{\boldsymbol{q}i}(\boldsymbol{r}) \psi_{k-\boldsymbol{q}l}(\boldsymbol{r}) \tag{17b}$$

$$\Phi_{\boldsymbol{q}i}(\boldsymbol{r}) = \sum U_{\boldsymbol{q}i}(\boldsymbol{G})\, \mathrm{e}^{\mathrm{i}(\boldsymbol{q}+\boldsymbol{G})\cdot\boldsymbol{r}} \tag{17c}$$

and

$$\langle \psi_{kn} | \Sigma^{\text{ex}} | \psi_{kn} \rangle = -\frac{1}{V} \sum_{\boldsymbol{q}}^{\text{BZ}} \sum_{n}^{\text{occ}} v(\boldsymbol{k}-\boldsymbol{q}) C^{kn}_{\boldsymbol{q}l}(\boldsymbol{G})^* C^{kn}_{\boldsymbol{q}l}(\boldsymbol{G}) \tag{18a}$$

$$C^{kn}_{\boldsymbol{q}l}(\boldsymbol{G}) = \sum_{\boldsymbol{G}'} \psi_{kn}(\boldsymbol{G}+\boldsymbol{G}') \psi_{\boldsymbol{q}l}(\boldsymbol{G}'). \tag{18b}$$

3. Numerical details

The calculations were carried out in momentum space. Wave functions were expanded in plane waves and for all the models studied it was found that 55 plane waves were

sufficient. The singularities in the Brillouin zone summations in the expressions for Σ^{corr} and Σ^{ex} were removed using the procedure proposed by Gygi and Baldereschi [33]. The expressions for the self-energy terms were further smoothed across the Fermi surface with a Fermi function, and the Brillouin zone summations for the smoothed functions were carried out using the special points method of Monkhorst and Pack [34]. The calculations were performed for a BCC structure and we used eight special points in the irreducible wedge of the Brillouin zone. Final results were accurate to $\simeq 0.1$ eV, which was deemed sufficient for the present qualitative study. In all the models an average charge density with density parameter $r_s \simeq 2.5$ au was used.

4. Results for model systems

In this section we present the results for a number of model potentials. In each case the total 'self-consistent' potential $V(r)$ in equation (14) was specified by up to three Fourier coefficients. With this small number of potential parameters, eigenvalues converged quickly with increase in the number of basis functions. Figures 1(*a*)–(*f*) summarise the results roughly in order of increasing inhomogeneity. The Fermi energy is at 0 eV in each case. The deviation of the density of states as a function of energy from a simple square root dependence is a measure of the inhomogeneity of the system. In figure 1 we also show graphs of the self-energy and the exchange and correlation energies (dots) calculated at a number of points within the irreducible wedge of the Brillouin zone as a function of the DFT eigenvalues for a number of systems with different densities of states. For comparison we plot the values for the corresponding quantities (full curves) for a homogeneous electron gas at the average charge density of the system.

It is immediately obvious that the self-energy of an inhomogeneous system is a sensitive function of both energy as well as wave vector and that this dependence becomes more evident for systems of greater inhomogeneity. From equation (16) it is obvious that within the approximations used in our calculations there exists a unique relationship between the quasiparticle energies and the self-energy matrix elements, but in figure 1 there is a scatter that arises from a dependence on the set of k-points at which the matrix elements are evaluated. The general trends remain, however, irrespective of the actual set of k-points chose. There is a wide scatter in Σ^{corr} and Σ^{ex} at similar energies, but the sum of the two terms is overal closer to the homogeneous electron gas values than the individual components. Deviation from the full curves in figure 1 is always in the opposite direction for Σ^{corr} and Σ^{ex} respectively. It is therefore important to treat Σ^{corr} and Σ^{ex} with the same accuracy in any calculation. The degree of cancellation of the two terms depends on the screened Coulomb potential and will change for different dielectric matrices, but the qualitative features are unlikely to be significantly affected by a more consistent model for the dielectric function.

From figure 1 it is clear that 'structure' in the density of states has important consequences for the self-energy matrix elements. In figures 1(*a*)–(*d*) there are two sets of points as the same DFT energies which can be related to a minimum in the density of states; these are not artifacts of the calculation. This is better demonstrated in figure 2 where the self-energy corrections to the DFT eigenvalues are plotted. The graphs in figure 2 correspond to the same models as considered in figure 1. For comparison we included a model with a gap in the density of states at the Fermi energy (figure 1(*f*) and figure 2(*f*)). Here there is a discontinuity in the self-energy correction for valence and conduction band states as found in more sophisticated calculations for semiconductors and

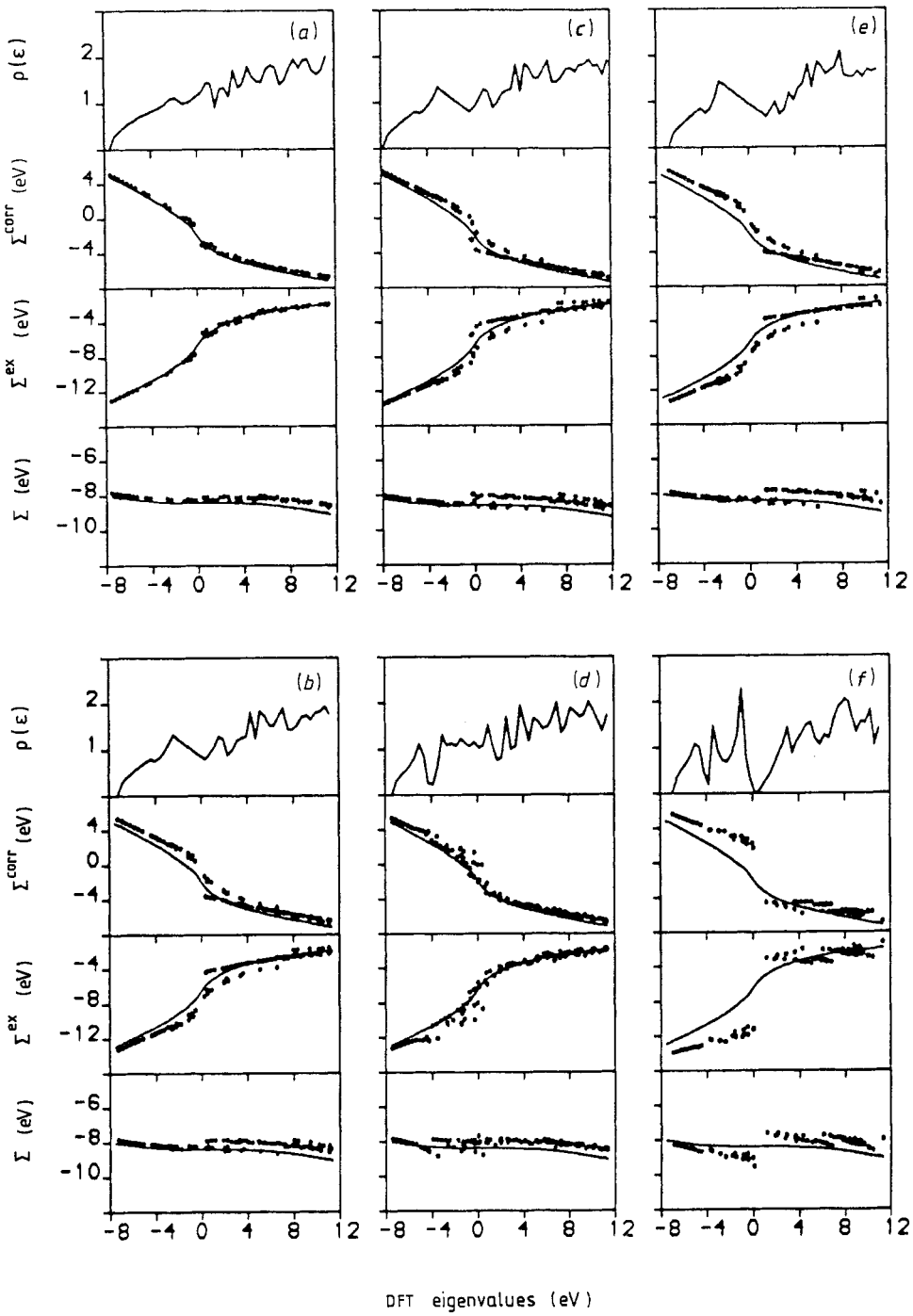

Figure 1. DFT density of states, correlation energy Σ^{corr}, exchange energy Σ^{ex} and self-energy Σ as a function of DFT eigenenergies for a number of model potentials. Dots—this calculation; full curves—homogeneous electron gas with average charge density of unit cell.

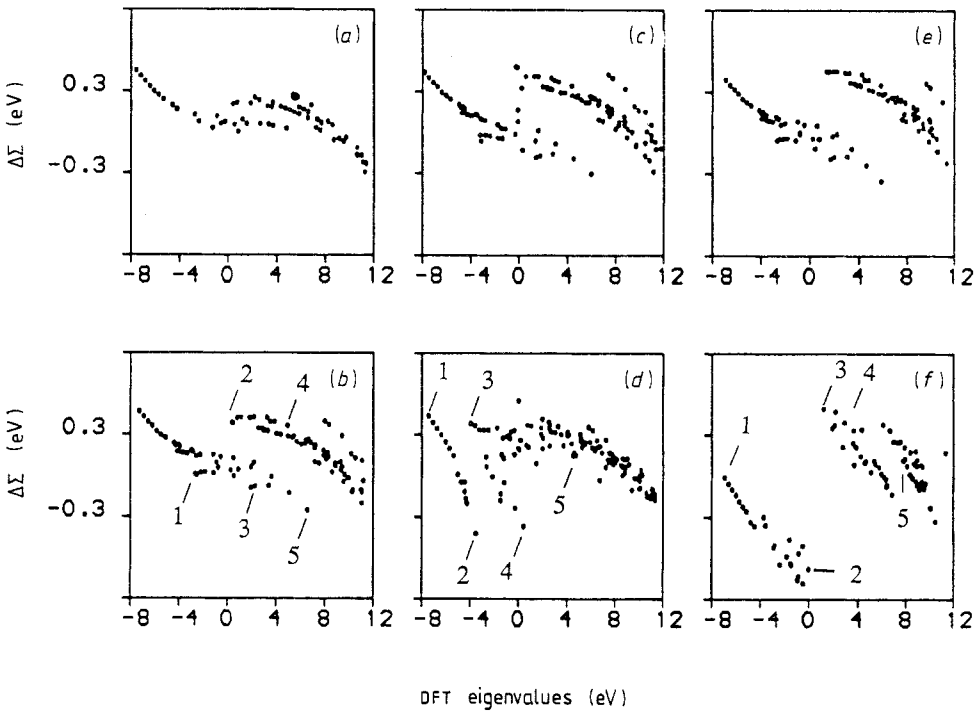

Figure 2. Self-energy correction to the DFT eigenergies for the same model potentials as in figure 1.

insulators [4–7], but in this instance the screened Coulomb potential is short range in contrast to the situation encountered in semiconductors and insulators. The feature found in figures 1 and 2(*a*), (*b*), (*c*) and (*e*)—that is, the two sets of self-energy points at the same DFT energies—is due to the symmetry of the states involved. In figures 3, 4 and 5 we show the ground-state charge density and partial densities $|\psi_\alpha(\boldsymbol{r})|^2$ for a selected number of states corresponding to the models shown in 1(*b*) (2(*b*)), 1(*d*) (2(*d*)) and 1(*f*) (2(*f*)) respectively. The numbers used to identify the partial densities refer to the corresponding numbers on the respective graphs in figure 2. It is clear that the set of points at lower energies in figure 2 in each case refer to states with high partial densities in the region of high ground-state charge density, and the points at higher energies relate to states with low partial densites of states in the region of high ground-state charge density. The states with bonding-like character—that is, states with a high partial density in the regions where the ground-state charge density is large—are depressed relative to states with less bonding-like character. This feature remains irrespective of whether the states are occupied or empty, as is clearly illustrated in figure 4 and figures 1(*d*) and 2(*d*). In this case there is a minimum in the density of states at $\simeq -3.5$ eV, with a discontinuity in the self-energy correction across this minimum. The discontinuity is not complete; the point numbered 2 in figure 2(*d*) lies at a DFT energy above the minimum in the density of states, but has bonding-like character (figure 4 (4)) and the self-energy correction is relatively large negative. The discontinuity in the self-energy in case (*f*) is a consequence of the difference in character of the states above and below the Fermi energy as illustrated in figure 5. This confirms the conclusion reached by von der Linden and Horsch [12] that

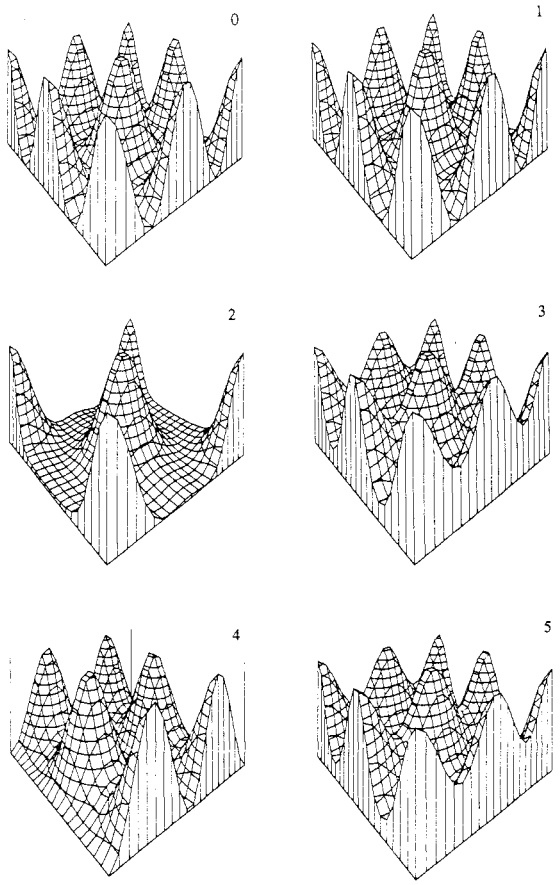

Figure 3. Ground-state charge density (0) and partial densities $|\psi_a(\boldsymbol{r})|^2$ (1–5) for selected states in the (110) plane. Arbitrary units are used. The numbers refer to the points indicated in figure 2(*b*).

the discontinuity in the self-energy across the band gap in semiconductors is closely related to the different symmetries of the valence and conduction band states. The potential used for figures 1(*b*) (2(*b*)) and 1(*c*) (2(*c*)) is the same, the only difference is that in 1(*c*) (2(*c*)) the Fermi energy lies at $\simeq$1 eV higher than in 1(*b*) (2(*b*)). The wave functions are therefore the same in both cases, but the charge density and consequently the dielectric matrix is different for the two situations. Careful comparison of the case again shows that the split in the self-energy is more sensitive to the properties of the wave functions than to the position of the Fermi level. This is also evident from the model shown in 1(*e*) (2(*e*)) where the split starts at the minimum in the density of states about 1 eV above the Frmi energy.

5. Summary and conclusions

We have shown that the self-energy potential for a metallic system within the GW approximation is a highly anisotropic function. The sign and relative size of the self-energy correction depends mainly upon the symmetry of the wave functions involved. As a rule of thumb, states with bonding-like character, that is with a high partial density in the regions of high ground-state charge density, are depressed relative to states with

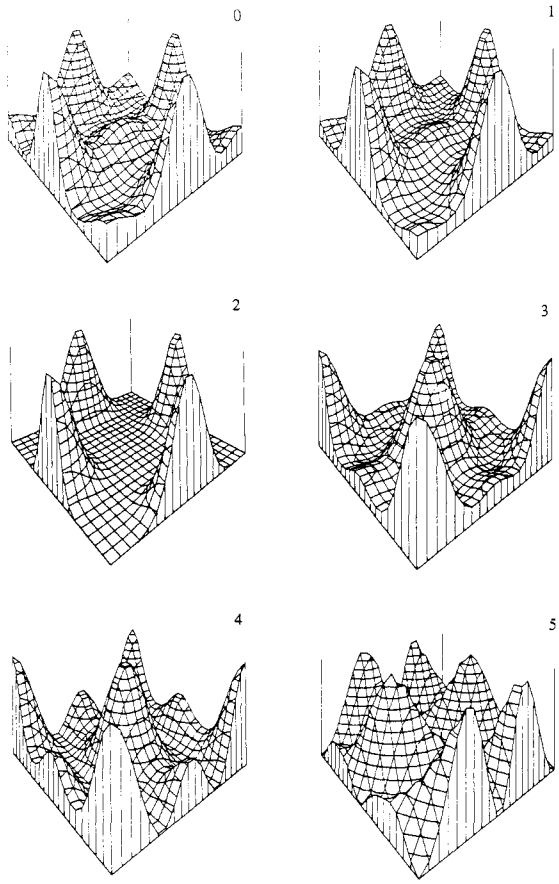

Figure 4. Ground-state charge density (0) and partial densities $|\psi_\alpha(\boldsymbol{r})|^2$ (1–5) for selected states in the (110) plane. Arbitrary units are used. The numbers refer to the points indicated in figure 2(*d*).

less bonding-like character. This can be important for metallic systems such as the BCC transition metals. For these systems [35] there is a minimum in the d-band density of states with the lower lying states mainly of E_{2g} character and the higher lying states of T_{3g} character. From the above work one would expect that for half filled d bands, the local minimum in the density of states will be enhanced by the self-energy correction. For occupied states the same situation may arise where states have different symmetry at different energy intervals as in 1(*d*) (2(*d*)). Lifetime effects though may wash out these features away from the Fermi energy. We have also confirmed that the discontinuity in the self-energy across the band gap found for semiconductors and insulators can occur even with a short range (metallic) screening potential; the discontinuity thus depends primarily on the different symmetry of the valence and conduction band states. In the model used for the dielectric matrix in this work it would be simple to replace the plasmon-pole approximation by an average over the dynamic Lindhard dielectric matrix for a homogeneous electron gas. This will considerably increase the computational requirements and is a project for the future, but we do not believe than any of the conclusions reached here would be altered.

The self-energy is intrinsically non-local in nature, but the relationship of the matrix elements and the partial densities of the wave functions suggest that it may be possible to construct an analytic local energy dependent potential which depends on the local

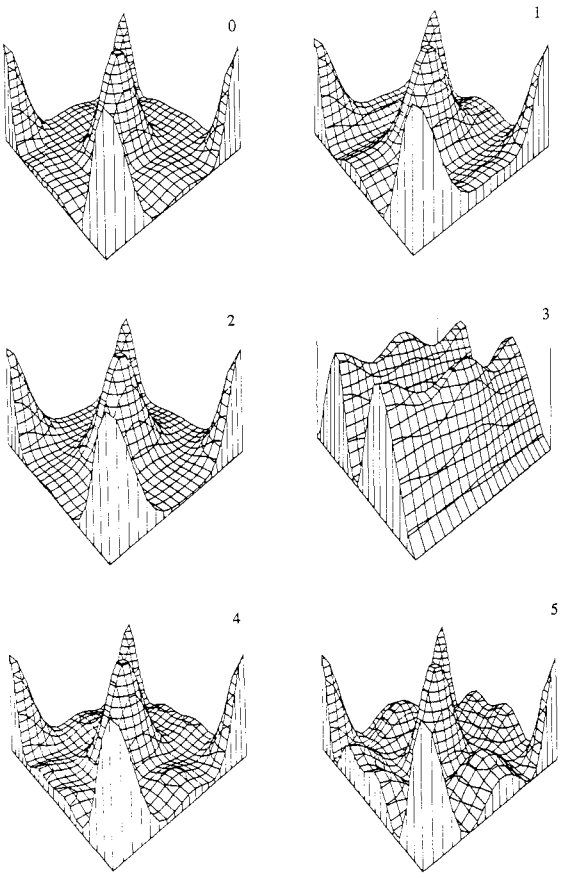

Figure 5. Ground-state charge density (0) and partial densities $|\psi_\alpha(\boldsymbol{r})|^2$ (1–5) for selected states in the (110) plane. Arbitrary units are used. The numbers refer to the points indicates in figure 2(f).

charge density for metallic systems. This has been done for semiconductors [36, 37] where model potentials that scale with the cube root of the charge density were constructed. The model potential of Hanke and Sham [37] has successfully been applied to a number of systems. The results presented in this paper show that it is essential to include an energy and wave-function dependent exchange and correlation potential in detailed calculations of electronic properties for metallic systems.

References

[1] Hohenberg P and Kohn W 1964 *Phys. Rev.* B **136** 1864
Kohn W and Sham L J 1965 *Phys. Rev.* **140** A1133
[2] Hedin L and Lundqvist S 1969 *Solid State Physics* vol 23 (New York: Academic)
[3] Perdew J P and Levy M 1983 *Phys. Rev. Lett.* **51** 1884
[4] Sham L J and Schlüter M 1983 *Phys. Rev. Lett.* **51** 1888
[5] Sham L J and Schlüter M 1985 *Phys. Rev.* B **32** 3883
[6] Lannoo M and Schlüter M 1985 *Phys. Rev.* B **32** 3890
[7] Godby R W, Schlüter M and Sham L J 1988 *Phys. Rev.* B **37** 10159
[8] Hybertsen M S and Louie S G *Phys. Rev.* B **34** 5390
[9] von der Linden W and Horsch P 1988 *Phys. Rev.* B **37** 8351
[10] Strinati G, Mattausch H J and Hanke W 1982 *Phys. Rev.* B **25** 2876

[11] Sterne P A and Inkson J C 1984 *J. Phys. C: Solid State Phys.* **17** 1497
[12] von der Linden W and Horsch P 1986 *Solid State Commun.* **59** 485
[13] Jensen E and Plummer E W 1985 *Phys. Rev. Lett.* **55** 1918
[14] Lyo I W and Plummer E W 1988 *Phys. Rev. Lett.* **60** 1558
[15] Lindgren S A and Walden L 1988 *Phys. Rev. Lett.* **61** 2894
[16] Citrin P H, Wertheim G K, Hafghizume T, Sette F, Macdowell A A and Comin F 1988 *Phys. Rev. Lett.* **61** 1021
[17] Lundqvist B I 1969 *Phys. Status Solidi* **32** 273
[18] Lundqvist B I 1967 *Phys. Kondens. Mater.* **6** 206
[19] Hedin L 1965 *Phys. Rev.* **139** A796
[20] Rice T M 1965 *Ann. Phys.* **31** 100
[21] Overhauser A W 1971 *Phys. Rev.* B **3** 1988
[22] Northrup J E and Louie S G 1987 *Phys. Rev. Lett.* **59** 819
[23] Surh M P, Northrup J E and Louie S G 1988 *Phys. Rev.* B **38** 5976
[24] Shung K W K, Sernelius B E and Mahan G D 1987 *Phys. Rev.* B **36** 4499
[25] Petrillo C and Sachetti F 1988 *Phys. Rev.* B **38** 3834
[26] Nakano A and Ichimaru S 1989 *Solid State Commun.* **70** 1989
[27] Mahan G D and Sernelius B E 1989 *Phys. Rev. Lett.* **23** 2718
[28] Wang C S and Pickett W E 1983 *Phys. Rev. Lett.* **51** 597
[29] Davis L C 1986 *J. Appl. Phys.* **59** R25
[30] Hybertsen M S and Louie S G 1987 *Phys. Rev.* B **37** 2733
[31] Baldereschi A and Tosatti E 1979 *Solid State Commun.* **20** 131
[32] Hedin L and Ludnqvist B I 1971 *J. Phys. C: Solid State Phys.* **4** 2064
[33] Gygi F and Baldereschi A 1986 *Phys. Rev.* B **23** 4405
[34] Monkhorst H J and Pack J D 1976 *Phys. Rev.* B **13** 5188
[35] Jepsen O, Andersen O K and Mackintosh A R 1975 *Phys. Rev.* B **12** 3084
[36] Stern P A and Inkson J C 1984 *J. Phys. C: Solid State Phys.* **17** 1497
[37] Hanke W and Sham L J 1988 *Phys. Rev.* B **38** 13361
[38] Kane E O 1971 *Phys. Rev.* B **4** 1910
[39] Inkson J C 1973 *J. Phys. C: Solid State Phys.* **6** L181